ELSEVIER

Journal of Nuclear Materials 266–269 (1999) 118–123

journal of nuclear materials

Operational limits for high edge density H-mode tokamak operation

W. Suttrop *, V. Mertens, H. Murmann, J. Neuhauser, J. Schweinzer, ASDEX-Upgrade Team

Max-Planck Institut für Plasmaphysik, Euratom Association, Boltzmannstrasse 2, D-85740 Garching, Germany

Abstract

Operational regime boundaries for High confinement mode (H-mode) plasmas with high edge density are investigated on the ASDEX Upgrade tokamak. In addition to the MHD stability boundary imposed by Edge Localized Modes (ELMs) and the H-mode threshold, the onset of complete divertor detachment limits the accessible separatrix density. At the H-mode density limit, a transport enhancement is observed that reduces the temperature gradient in the edge of the main plasma and can lead to a disruption by loss of H-mode and and subsequent radiation and resistive MHD instability. This 'transport limit' occurs parallel to full divertor detachment at high edge collisionalities. A possible origin is drift-Alfvén-ballooning turbulence driven by the pressure gradient at high collisionality.

Keywords: High-confinement mode; Density limit; Edge localized modes; Divertor detachment; Plasma edge; Tokamak; Nuclear fusion

1. Introduction

It is desirable to achieve high edge density in a tokamak which facilitates power removal within the narrow margins of impurity content permissible in a nuclear fusion plasma. At the same time it is necessary to maintain good H-mode confinement to achieve fusion burn in a machine with reasonable size. For this reason, the H-mode density limit is extensively studied on ASDEX Upgrade [1]. A density limit close to the Greenwald limit $\bar{n}_{GW}$ is found in H-mode which is almost independent of heating power. Near the density limit, the heating power needed to maintain H-mode strongly increases in contrast to the usual $P \propto \bar{n}_e B_t$ scaling of the H-mode threshold. In the present paper, we investigate the physics mechanisms that lead to the H-mode density limit and the strong increase of the H-mode threshold.

It has been shown [2] that several operational boundaries (H-mode transition, ELM type, ballooning stability, radiation stability) are governed by plasma edge parameters, in particular temperature, density and pressure gradient at the separatrix or in the H-mode barrier region (a few cm inside the separatrix). In particular, a fundamental density limit for H-mode is imposed by the pressure gradient limit due to ELMs, which can reduce the temperature in the pedestal region at high edge density to below the H-mode threshold, which appears as an edge temperature threshold at high densities [2]. In this picture, the edge density during H-mode can be raised until the ELM pressure gradient limit reduces the edge temperature to below the H- to L-mode threshold. Experimentally, this fundamental limit is not reached, because additional effects become important. The onset of divertor detachment imposes a limit on the separatrix density (Refs. [3,4] and references therein). This limit by itself is not disruptive. Nevertheless, H-mode density ramp experiments usually lead to a back-transition to L-mode, MARFE expansion on closed flux surfaces, edge cooling and a disruption caused by resistive MHD instability [1]. In the following it will be shown that the H–L back-transition is related to a decreased edge temperature gradient which develops in parallel with increasing degree of detachment and is

* Corresponding author. E-mail: suttrop@ipp.mpg.de

0022-3115/99/$ – see front matter
PII: S 0 0 2 2 - 3 1 1 5 (9 8) 0 0 5 7 3 - X

interpreted as a signature of enhanced radial transport, or deterioration of the H-mode barrier.

Experiments are performed in ASDEX Upgrade with the new tightly baffled divertor II [5], pumped by 13 turbo-molecular pumps with a pumping speed of 1000 l/s each. Heating powers P_{heat} up to 7.5 MW neutral beam injection (NBI) and 2 MW ion cyclotron heating (ICRF) are used for the present investigation. The plasmas are fuelled by deuterium gas puffing, either into the divertor or the main chamber. The results presented here are found not to depend on the location of the gas source. All H-modes in ASDEX Upgrade show ELMs which result in quasi-stationary density and temperature profiles. Slow P_{heat} and gas puff ramps are applied to obtain a controlled increase of density in H-mode. Edge parameters are measured with the Li-beam (edge density) and the Thomson scattering (edge temperature) systems. High spatial resolution is achieved by combining successive shots of radially displaced lasers into single profiles.

2. Edge density limit by divertor detachment

First we demonstrate that a separatrix density limit is encountered simultaneous with divertor detachment using an H-mode discharge in ASDEX Upgrade as an example. Fig. 1 shows time traces of heating power, core radiation, divertor CIII (C^{2+}) intensity ($\lambda = 465$ nm) from sightlines that intersect the outer divertor plates near the strike point and a few centimeters above the strike point as a measure of power flux to the divertor, line averaged and separatrix densities, edge temperature and total stored energy. The density set point is quickly

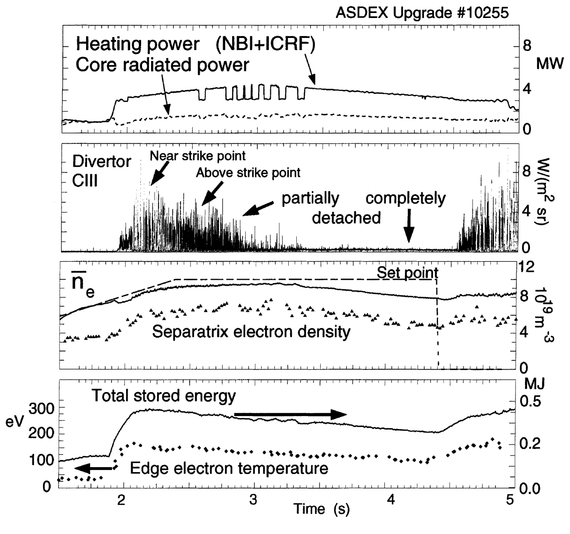

Fig. 1. Example of edge density limit with the onset of complete divertor detachment.

ramped up and then held at $\bar{n}_e = 80\% \; \bar{n}_{GW}$. As this density is never reached in the discharge, the gas valves remain fully open from $t = 1.95$ to 4.4 s (deuterium gas puff rate: $1.3 \times 10^{22} \; s^{-1}$). The heating power (constant NBI power plus ICRF power ramp from 1.9 to 4.8 s) is first ramped up. During this phase the line averaged and separatrix densities increase, and a drop of the CIII signal near the strike point indicates the onset of partial detachment. After $t = 3$ s, the heating power is slowly ramped down. At $t = 3.4$ s the peripheral CIII signal drops as well indicating that the divertor becomes fully detached. The edge density drops significantly from 7×10^{19} to 5×10^{19} m^{-3} at $t = 4.4$ s when the gas valves close and the discharge reverts to an attached state. Note that since the power ramp is done by ICRF heating, there is no change of beam fuelling. The edge electron temperature as well as the total stored energy are highest in the initial attached phase and deteriorate with increasing degree of detachment. The energy confinement time, corrected for the change of stored energy $\tau = W_{tot}/(P_{heat} - dW_{tot}/dt)$, drops with increasing density until $t = 3.0$ s and then remains approximately constant until $t = 4.4$ s.

Reconstruction of 2D radiation profiles from bolometer measurements show that during partial detachment [$t = 2.5$ s, Fig. 2(a)], like in the attached case, divertor radiation is confined to a region near the strike points in the inner and outer divertors. In the fully detached phase [$t = 4.0$ s, Fig. 2(b)], the radiating zone is spread over the entire outer divertor leg which carries most of the power flux, indicating a divertor temperature near or below 10 eV in the entire outer divertor. It should be noted that throughout this particular discharge, the inner and outer strike points are detached in between ELMs. Generally, detachment in between ELMs sets in already at densities below the density limit. Detachment during ELMs seems to coincide with the loss of large type I ELMs, which carry about 40% of the power flux across the separatrix practically independent of ELM frequency and plasma parameters [6].

3. Transport enhancement at the plasma edge

A second observation at high edge densities is the reduction of edge gradients with the onset of detachment. This is demonstrated in Figs. 3 and 4 for another ASDEX Upgrade discharge with higher heating power than the previous example. The heating power is quickly ramped up to obtain H-mode with type I ELMs and simultaneously a strong gas puff begins. With increasing neutral gas flux [Fig. 3(a)] the ELM frequency becomes irregular and large ELMs interspersed with quickly repeating ELMs appear. We refer to this phenomenon here as ‘mixed’ ELM types and interpret it as type I ELMs due to which the edge temperature drops below

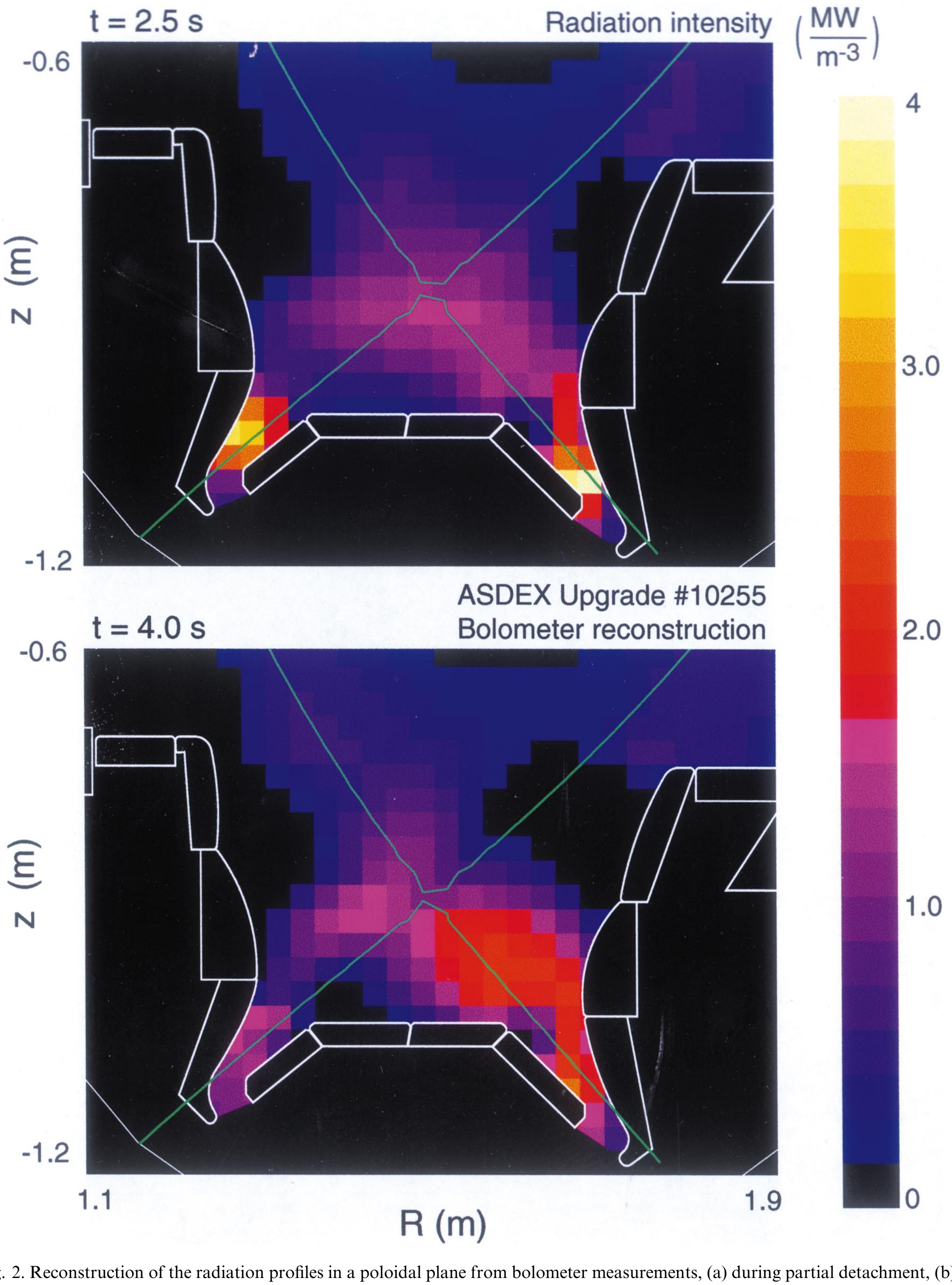

Fig. 2. Reconstruction of the radiation profiles in a poloidal plane from bolometer measurements, (a) during partial detachment, (b) at full detachment.

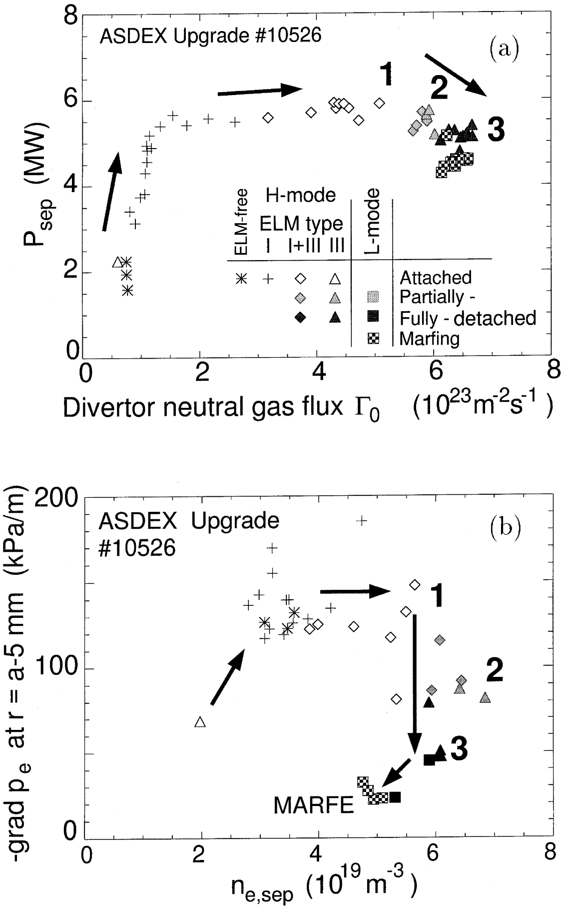

Fig. 3. Trajectories showing the relation between divertor detachment and four parameters in a P_{heat} ramp-down experiment (a) in $P_{sep}/\Gamma_{0,div}$ space, (b) in grad $p_e/n_{e,sep}$ space. The various symbols denote attached, partially and fully detached phases as well as L-mode and H-mode with various types of ELMs (see figure inset). The numbers indicate phases in the transition from attached conditions (1) to partial (2) and full detachment (3), which is followed by MARFE formation.

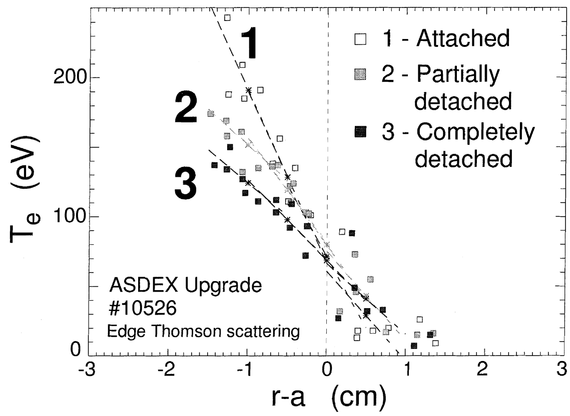

Fig. 4. Edge electron temperature profiles during the transition from the attached (1) to partially (2) and fully detached state (3) of Fig. 3. The separatrix temperature remains approximately constant, but the temperature gradient decreases steadily.

the temperature threshold for type III ELMs to become unstable [2]. During this phase, the divertor begins to detach and irregular and fast type III ELMs appear. As the heating power (and separatrix power) is ramped down, and the neutral gas flux increases, the divertor becomes fully detached. After the H–L transition, the midplane separatrix temperature drops and a MARFE forms. Fig. 3(b) shows that following the path from onset of partial detachment (1) to onset of complete detachment (2) to just prior to the H–L transition (3), the edge density does not increase significantly despite the increasing neutral gas flux, and at the same time the edge pressure gradient drops. This is due to a drop of the edge temperature gradient, as shown in Fig. 4. The T_e profiles pivot around an almost constant temperature T_{sep} at the separatrix, $r = a$, consistent with a weak power dependence $T_{sep} \propto P^{2/7}$ combined with the small change of P_{sep}. Given the small variation of P_{sep} and the constant edge density, we can interprete this reduction of the edge T_e gradient as an increase of the effective perpendicular electron heat diffusion coefficient, defined as $\chi^*_{e,\perp} = -P_{sep}/(n_e \text{ grad } T_e)$. It is important to note that although $\chi^*_{e,\perp}$ increases strongly at the plasma edge, this has no immediate effect on the global energy confinement time. The deleterious nature of the transport enhancement is to reduce the edge temperature and, if the gas puff is not reduced nor the heating power strongly increased, to create MARFE instability and a disruption. Also, divertor detachment by itself does not lead to core confinement deterioration. An example is the Completely Detached H-mode (CDH mode) [7], where controlled edge radiation by neon injection leads to detachment in type III ELMy H-mode while the H-mode confinement is at or above the level of type I ELMy H-modes.

4. Summary and discussion

The experimental observations described above lead to the following picture of the H-mode density limit: For any given edge density profile, the edge temperature gradient is limited by the pressure gradient limit imposed by type I ELMs. Thus, the edge temperature in the H-mode barrier and the H-mode pedestal must decrease with increasing edge density. With decreasing temperature or increasing collisionality, the ELM type changes first from type I ELMs to type I ELMs with intermittent type III ELMs ('mixed ELMs') and finally to type III ELMs. Type III ELMs are destabilized below a certain edge temperature and occur at various edge pressure gradients up to the type I ELM limit [2]. Detachment sets in first in between ELMs. Experimentally, during type I ELMs the inner and outer divertors are at least partially attached. Complete detachment as measured by the power flux to the target plate (CIII intensity) begins at high edge densities after type I ELMs have disappeared and only type III ELMs occur. In this phase, the separatrix density remains constant or drops slightly regardless of the further increase of neutral gas flux. We attribute this saturation to be a consequence of a detachment density limit according to the mechanism outlined in Refs. [4,3] and illustrated with examples in JET in Ref. [4].

Simultaneous to the transition to complete detachment, the edge pressure gradient drops. From the observation of these concurrent phenomena, no cause-consequence relation can be directly inferred. One can conceive of several possibilities.

First, detachment leads to a strongly increased neutral flux from the divertor to the main chamber which could affect radial transport inside the separatrix, if a sufficient neutral density can be built up. Although the present divertor II in ASDEX Upgrade is pumped from the private flux region, this region is baffled against the X-point so that the path for neutrals to enter the core plasma via the private flux region towards the X-point is only accessible when the entire divertor chamber is cold and transparent to neutrals. In this case the neutral flux towards the X-point can increase by several orders of magnitude compared, e.g. with the midplane neutral flux, but due to large flux expansion in the X-point region the penetration depth (in flux coordinates) is also much smaller than at midplane. It depends on details of the density and temperature distribution around the X-point whether the neutral penetration is significant compared to that in other regimes (attached divertor, L-mode, low density H-mode etc.) and can cause a change of transport. However, calculations on ASDEX Upgrade [1] show that with increasing scrape-off layer density, the velocity shear region just inside the separatrix becomes better shielded from penetrating neutrals because of the higher ionization probability. A comparison of neoclassical viscosity and neutral friction [8] shows that the damping of the poloidal rotation by neutrals is negligible. The damping of the toroidal rotation is small and it depends on possible competing mechanisms whether the neutrals can have an appreciable effect on the radial electric field.

An alternative explanation of the drop of the T_e gradient can be a change of perpendicular transport in the H-mode barrier region by a mechanism independent of detachment or divertor physics. As the transport increase is seen at high density below the MHD pressure gradient limit, this hypothesis invokes a dependence of transport coefficients, e.g., on edge collisionality, or edge temperature or it may be connected to the change of edge MHD activity from type I to type III ELMs. In this picture, the onset of detachment, which also occurs at high collisionality, would be either coincidental with the change of radial transport or could be driven by an accompanying increase of $\chi_\perp$ in scrape-off layer.

Recently, simulations of anomalous radial transport at the plasma edge based on three-dimensional Drift-Alfvén [9] and Drift-Ballooning [10] models have been reported. Many features of the simulation results seem to depend on details of the models employed. However, a common result is that radial transport increases strongly with increasing normalized pressure $\hat{\beta} = \beta(qR/L_\perp)^2$ [9] or pressure gradient $\alpha = -Rq^2\,\mathrm{d}\beta/\mathrm{d}r$ [10] and increases with increasing collision frequency ν [9] (at fixed β). A particular property of the model proposed in Ref. [10] is that depending on the so-called "diamagnetic parameter" α_d, which is essentially a measure of collisionality, $\alpha_d \propto \nu^{*^{-1/2}}$, the radial fluxes either increase (low α_d, high collisionality) or decrease (large α_d, low collisionality) with α. The latter effect is a result of finite-β stabilization of the driftwave turbulence with increasing α in combination with self-generated $E \times B$ shear flow due to the turbulence and has been proposed as a possible cause for the transport reduction in H-mode [10]. The bifurcating character of the H-mode arises because power and particle fluxes are the slowly varying control parameters, and the profile steepening by reduced transport at fixed fluxes supports the transport reduction.

In Ref. [10], an operational space diagram is given in (α_d, α)-space. We can test if measured plasma edge parameters in ASDEX Upgrade reproduce the main features of the transport model (Fig. 5). We plot only the electron part of α_e, as edge T_i measurements with suffi-

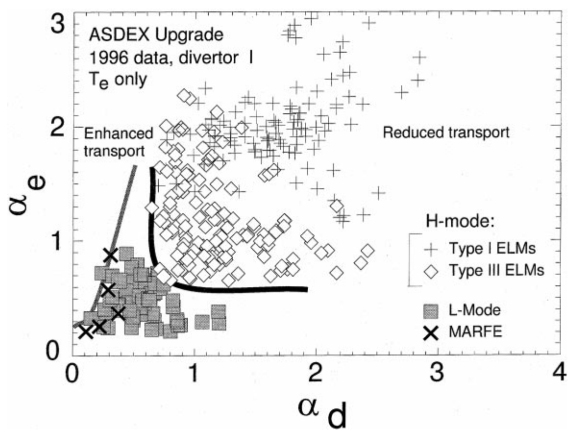

Fig. 5. ASDEX Upgrade (divertor I) edge α_e (normalized electron pressure gradient) vs. edge α_d (diamagnetic parameter) for the data set of Ref. [2]. Except for a difference in scale of α_d, transport reduction (H-mode) and radiation instability are found near the boundaries predicted in Ref. [10]

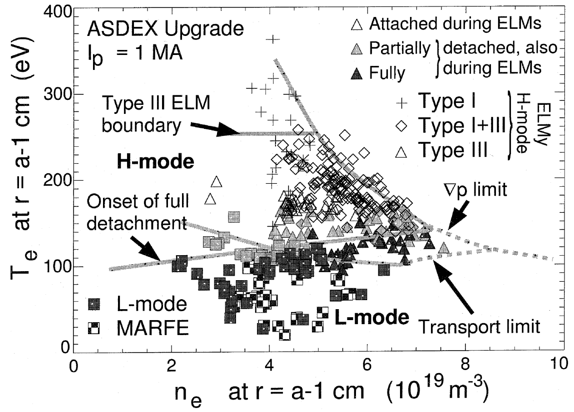

Fig. 6. Extended edge operational diagram including the onset of partial and complete detachment during ELMs and the transport limit. The data points are combined trajectories in T_e/n_e space (data taken at $r = a - 1$ cm) during eight discharges with different P_{heat} and gas puff trajectories but same toroidal field ($B_t = 2.5$ *T*) and plasma current ($I_p = 1.0$ *MA*). The various edge-related operational boundaries discussed in the text are schematically marked.

cient resolution and accuracy are only available for a limited number of discharges. The data is taken at $r = a{-}1$ cm, all gradients are finite differences between data points at $r = a$ and $r = a{-}2$ cm. The data set contains stationary L-mode, type I and type III H-mode phases of the divertor I phase of ASDEX Upgrade with both hydrogen and deuterium gas, $B_t = 1.5$–2.7 T, $I_p =$ 0.6–1.2 MA, and both magnetic field directions. The full lines indicate the onset of enhanced transport (left) and transport reduction (right). One sees that these limits coincide well with the boundaries predicted in Ref. [10]. One should note that the absolute value of α_d depends on the radial position at which the data is taken. In L-mode, the normalized electron pressure gradient α_e alone reaches the ideal MHD stability limit predicted in the calculation. As generally $T_i \geqslant T_e$ for the NBI heated discharges shown, the total α is somewhat above the predicted limit as calculated for toroidal geometry with elongation $\kappa = 1$ and triangularity $\delta = 0$. For $\alpha_d > 1$, this limit is lifted because the ideal MHD mode is stabilized by $E \times B$ shear flow and ion diamagnetic effects in line in with the observation of larger α_e in H-mode.

We can now extend the edge operational diagram in boundary T_e/n_e space introduced in [2] with the detachment and transport limits (Fig. 6). A position at $r = a - 1$ cm is chosen which can be diagnostically covered also at higher densities. The data points represent measurements during eight H-mode discharges in deuterium with $I_p = 1$ MA and $B_t = 2.5$ T, and with different gas puff and heating power trajectories in order to trace out the path to high edge density. In addition to the H-mode threshold, the type III ELM boundary, the ELM-induced pressure limit and the boundary of radiation instability, the onset of full power detachment (in between and during ELMs) and the proposed onset of transport enhancement (for the maximum $P_{heat} = 8$ MW applied) are plotted schematically. One sees from the experiments that the latter two limits may approximately be represented by curves of constant collisionality, $T_e \propto \sqrt{n_e}$, which is an expression of the co-linearity of these effects.

We investigated density ramps in discharges with varying plasma current from $I_p = 0.6$ to $I_p = 1.2$ MA with constant q to study the effect of changed pressure gradient limit. The phenomenology of the H-mode density limit is similar to the examples at $I_p = 1$ MA shown. The onset of detachment occurs roughly along the boundary indicated in Fig. 6. The variation of the MHD limit corresponds to a variation of the maximum separatrix density which is found to be in approximate agreement with the Greenwald scaling.

In summary, we have shown that in addition to ELM induced MHD stability and the H-mode boundary, divertor detachment and an increase of edge transport at high collisionalities limit the H-mode edge density. Thereby, for essentially flat density profiles obtained by edge fuelling, also the accessible core density is limited. It is not clear so far why the boundaries of detachment and transport increase appear co-linear and whether a causal relation exists. Further studies, including an inter-machine comparison, and plasma parameter scans are desirable to test this co-linearity and clarify its origin.

References

[1] V. Mertens, M. Kaufmann, J. Neuhauser et al., Nucl. Fusion 37 (1997) 1607.

[2] W. Suttrop, M. Kaufmann, H.J. de Blank et al., Plasma Phys. Control. Fusion 39 (1997) 2051–2066.

[3] K. Borrass, R. Schneider, R. Farengo, Nucl. Fusion 37 (1997) 523–537.

[4] K. Borrass, J. Lingertat, R. Schneider, Contrib. Plasma Phys. 38 (1998) 130–136.

[5] R. Schneider et al., these Proceedings.

[6] W. Suttrop et al., Plasma Phys. Control. Fusion 40 (1998) 771.

[7] O. Gruber et al., Phys. Rev. Lett. 74 (1995) 4217.

[8] A.G. Peeters, J. Stober, D. Coster, Plasma Phys. Control. Fusion 40 (1998) 703.

[9] B. Scott, Plasma Phys. Control. Fusion 39 (1997) 1635–1668.

[10] B.N. Rogers, J.F. Drake, A. Zeiler, Phase Space of Tokamak Edge Turbulence, the L–H Transition, and the Formation of the Edge Pedestal, Phys. Rev. Lett. (submitted) ; B.N. Rogers, J.F. Drake, Phys. Rev. Lett. 79 (1997) 229.